Effective Age of Information in Real-Time Wireless Feedback Control Systems

Bo Chang[1,2], Burak Kizilkaya[1*], Liying Li[3], Guodong Zhao[1], Zhi Chen[2] & Muhammad Ali Imran[1]

[1]*School of Engineering, University of Glasgow, Glasgow* G12 8QQ*, UK;*
[2]*National Key Lab. on Communications, University of Electronic Science and Technology of China (UESTC), Chengdu* 611731*, China;*
[3]*Department of Mathematics, Physics and Electrical Engineering, Northumbria University, Newcastle upon Tyne* NE1 8ST*, UK*

Abstract *Ultra-reliable and low-latency communication* (URLLC) is one of the most important scenarios in forthcoming fifth generation (5G) cellular networks to ensure timely exchange of information and realize real-time wireless control. In URLLC, timely information update needs to be guaranteed since control performance, e.g., control cost and stability, is directly determined by timely control information update. In this paper, we introduce an *effective age of information* (EAoI) to evaluate the timeliness of information update in control process. We consider the control process with two phases: sensor to controller phase and controller to actuator phase. We adopt FGFS $M/M/1/1 \rightarrow M/M/1/2$ and FGFS $M/M/1/1^* \rightarrow M/M/1/2^*$ tandem queuing models to represent control process and we use finite-state Markov Chains to describe control information updates. By studying state transitions, we calculate the average EAoI for both tandem queuing models. More importantly, we analyze throughput of wireless control systems and its relationship with average EAoI, which provides a guideline for URLLC system design in real-time feedback control systems. Simulation results show the advantage of using EAoI.

Keywords Age of information, Communications, Feedback control, Queuing, Throughput, URLLC

Citation Chang B, Kizilkaya B, Li L, et al. Effective Age of Information in Real-Time Wireless Feedback Control Systems.

1 Introduction

The real-time wireless feedback control is a primary feature in many emerging application areas such as Cyber-Physical Systems (CPS), Industrial Internet of Things (IIoT), and tactile internet [1][2] where *ultra-reliable and low-latency communication* (URLLC) [3–7] is critical to ensure real-time control performance, e.g., control cost and stability. As shown in Fig. 1, a typical real-time wireless feedback control system consists of two phases [8–13], i.e. Phase 1 from sensor to controller and Phase 2 from controller to actuator. To ensure system performance and stability, one of main requirements is the timely exchange of information between the two phases.

In Phase 1, the sensor measures the status of the plant and transmits updates to the controller via URLLC. This process is called status update and the timeliness of status update is measured by Age of Information (AoI) [14]. AoI is the amount of time elapsed since the moment that the freshest received update was generated. Current studies [15] on AoI generally consider status update, i.e. Phase 1. On the other hand, in Phase 2, the controller collects status updates and creates control commands accordingly. Then, it transmits control commands to the actuator to be executed. This process is called actuation update and timeliness of actuation update is studied in [18].

However, how to obtain AoI for the whole control process from sensor to actuator via controller is still open and challenging. This is because the two phases in the control process are interdependent, where the failure of one phase will lead to invalidation of the other phase. Therefore, the whole control process should be treated as an end-to-end (E2E) link [10] rather than two independent links. Accordingly, in

* Corresponding author (email: b.kizilkaya.1@research.gla.ac.uk)

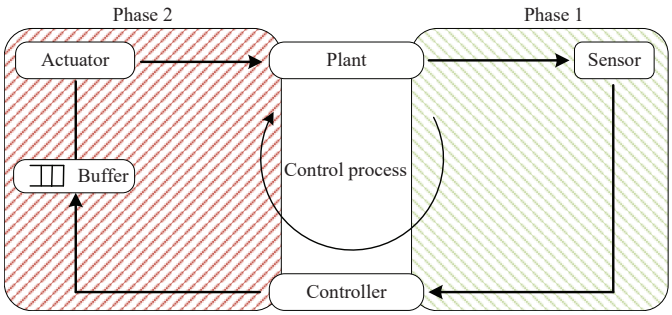

Figure 1 A typical real-time wireless feedback control system with URLLC.

the calculation of AoI for the whole control process, we need to consider E2E link rather than directly adding the AoIs of two phases.

In this paper, we define Effective Age of Information (EAoI) which considers the whole control process from sensor to actuator as shown in Fig. 1. The goal is to obtain the closed-form expression for the EAoI by tracking the whole control process. To achieve this goal, the key is to find suitable queuing models which represent the whole real-time feedback control process. Then, EAoI can be obtained by $\Delta(t) = t - L(t)$, where t represents the observation time at actuator and $L(t)$ represents the generated time of the latest sampled packet at sensor. Here, the main contributions of this paper are summarized as follows:

- We define EAoI, which is the time elapsed from the generation time of the last successful control process update until the time that current successful control process update is executed. This time duration is affected by sampling period, time delay, and packet loss which are critical parameters affecting control performance.
- We introduce two general first-generate-first-serve (FGFS) tandem queuing models according to the procedure of the control process. By studying state transition of finite Markov chain for the adopted tandem queuing models, closed-form expressions of EAoI for real-time wireless feedback control system are obtained.
- We analyze throughput for the real-time wireless feedback control system based on average EAoI. Then, we discuss the relationship between EAoI-based throughput and parameters in the tandem queuing models, which gives a guideline for URLLC system design.

1.1 Related Work

The AoI was firstly introduced in 1990s in real-time database systems to ensure the freshness of data [16] [17]. It is used as a metric to compare different synchronization techniques for databases. In recent years, queuing theoretic approach is introduced in AoI research to analyze the age metric in various kinds of systems [15]. AoI became more important with the development of new technologies such as Internet of Things (IoT), smart cities, Ultra-Reliable Low-Latency Communication (URLLC), remote control systems and so on.

The current research on AoI usually considers source-to-destination link in sensor networks [14, 19–23]. For instance, the authors in [14] discussed the calculation of average AoI and peak AoI in direct source-to-destination link with different queuing models. In [19], the authors minimized AoI of status update for FGFS source-to-destination link by optimizing the arrival rate.

Moreover, there are other works which consider AoI for source-to-destination link in specific scenarios [24–30]. For instance, the authors in [24] considered an energy harvesting source and optimized the AoI penalty in status update. In [26], the authors introduced the AoI into content update in a local cache, where they found that update rate in the cache is proportional to the square-root of items' popularity.

Furthermore, other works have been done on wireless control systems [31–33]. For instance, the authors in [31] studied the usage of AoI in centralized scheduling problem for the real-time networked control with source-to-destination link. In [32], authors applied AoI to wireless scheduling problem for networked control systems. In [33], authors studied the impact of random AoI on the performance of cyber physical control systems. However, the above studies cannot be used to describe the whole control process in real-time wireless feedback control systems since sensor-to-controller and controller-to-actuator links are

interdependent. In addition, these studies does not provide AoI definition for real-time wireless feedback control systems. They use conventional AoI definition.

The works that are most relevant to this paper are [34] and [35], where the authors analyzed the average AoI with a last-generate-first-serve (LGFS) tandem queuing model or multi-source queuing model in sensor networks since latest data is critical for sensor networks. However, the LGFS model cannot be used in real-time wireless feedback control systems since the control stability is determined by the ordinal data, which cannot be maintained by LGFS queuing model. On the contrary, the FGFS model is an exact match considering the process of real-time wireless feedback control. Furthermore, the AoI calculation methods in [34] and [35] cannot be used for FGFS model. This is because the packet discard strategies are significantly different between LGFS and FGFS models, where the previous packet should be discarded when the new packet comes for LGFS model while it is exactly opposite for FGFS model.

Considering existing literature, AoI definition for real-time wireless feedback control systems considering the whole control process from sensor to actuator via controller is still open and challenging problem. Accordingly, the calculation of AoI for the whole control process is missing. Therefore, we proposed the novel timeliness metric called EAoI for real-time wireless feedback control systems. We have also provided calculation of EAoI as well as analyzed throughput based on proposed new metric EAoI which provide foundation for further studies.

1.2 Organization

The rest of this paper is organized as follows. In Section II, the system model and the EAoI definition are presented. In Section III, the average EAoI is analyzed. In Section IV, the throughput for the real-time wireless feedback control systems is presented based on EAoI. In Section V, simulation results are provided to demonstrate the performance. Finally, Section VI concludes the paper.

2 System Model and Problem Statement

As shown in Fig. 1, we consider AoI and system throughput in a typical real-time wireless feedback control system [36][37]. In such a system, the whole control process has two phases:

- Phase 1: the sensor takes samples of a plant, and sends them to the remote controller, where the corresponding control commands are calculated;
- Phase 2: the controller transmits control commands to the actuator. Then, the actuator executes the control commands, and updates plant state.

Based on the above two phases, we introduce the definition of *effective age of information* (EAoI) for each update in control process.

Definition 1 (*Effective age of information for control process*): *For each update in control process, the effective age of information is defined by*

$$\Delta(t_k) = t'_k - t_{k-1}, \tag{1}$$

where t'_k represents the time instant when the actuator finishes Phase 2 for the k-th control command, and t_{k-1} represents the time instant when sensor starts Phase 1 for the $(k-1)$-th update. ■

Note that control performance, e.g., control cost or control stability, is closely related with EAoI, i.e., the time duration between t_{k-1} and t'_k. This time duration consists of sampling period of two contiguous successful control processes and time delay from sampling time instant to performing time instant of the corresponding control command at the actuator for each control process. This means that three critical parameters affecting control performance, i.e., sampling period, time delay, and packet loss [12], are indicated by EAoI. Thus, the proposed EAoI in this paper is critical for real-time wireless feedback control systems.

To calculate EAoI for each update in control process, we consider two typical tandem queuing models, i.e., FGFS $M/M/1/1 \rightarrow M/M/1/2$ tandem queuing model and $M/M/1/1^* \rightarrow M/M/1/2^*$ tandem queuing model, where the samples generated at the sensor follow Poisson process with parameter λ, the update time for Phase 1 and Phase 2 are exponentially distributed with update rate μ_1 and μ_2, respectively.

In FGFS $M/M/1/1 \rightarrow M/M/1/2$ tandem queuing model, for Phase 1, the new arrival samples are discarded when the controller is busy; otherwise, they would be immediately transmitted and served by

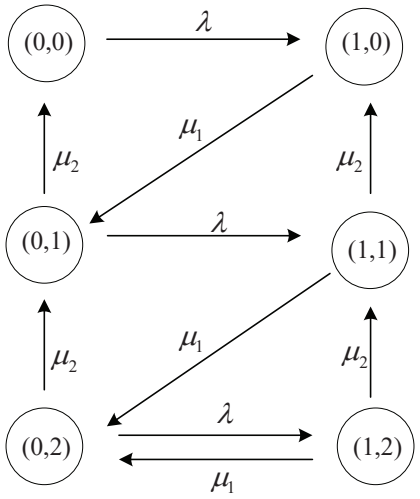

Figure 2 SHS Markov chain for $M/M/1/1 \rightarrow M/M/1/2$ tandem queue.

the controller. For Phase 2, a single control command packet would be kept when either condition in the following is satisfied:

- the actuator is idle;
- the actuator is busy, and the buffer is idle.

Otherwise, it would be discarded.

In FGFS $M/M/1/1^* \rightarrow M/M/1/2^*$ tandem queuing model, for Phase 1, the new sampled packet would be immediately transmitted and served by the controller. For Phase 2, a new control command packet would be served immediately when the actuator is idle, or would be kept in the buffer when the actuator is busy, or would replace the one that waits in the buffer when both the actuator and buffer are busy.

Based on the above system model and statements, we discuss the average EAoI calculation for control process update in the next section.

3 Average Effective Age of Information in Real-Time Wireless Feedback Control Systems

In this section, we first discuss the average EAoI for control process with FGFS $M/M/1/1 \rightarrow M/M/1/2$ tandem queuing model in real-time wireless feedback control systems. Then, we analyze the average EAoI for control process with FGFS $M/M/1/1^* \rightarrow M/M/1/2^*$ tandem queuing model.

3.1 Average EAoI for FGFS M/M/1/1 → M/M/1/2

The states of FGFS $M/M/1/1 \rightarrow M/M/1/2$ tandem queuing model are $(0,0)$ $(1,0)$ $(0,1)$ $(1,1)$ $(0,2)$ and $(1,2)$, where the first and the second entry represents the states in Phase 1 and Phase 2, respectively. For instance, the first entry indicates the state of Phase 1, i.e., 0 means Phase 1 is idle and 1 means it is busy. The second entry indicates the state of of Phase 2, i.e., 0 means that both actuator and buffer in Phase 2 are idle, 1 means actuator is busy and buffer is idle, and 2 means both actuator and buffer are busy.

The transition of the aforementioned states can be used in EAoI calculation, which can be described by a stochastic hybrid system (SHS) Markov chain as shown in Fig. 2 [38]. For example, the state $(0,0)$ in Fig. 2 would transfer to $(1,0)$ with rate λ when a new sampling packet is generated at the sensor. Other transitions in Fig. 2 is similar with the above example when a new sample or a new control command is generated[1)].

Let S_i represent the system state when the i-th sampling packet arrives at the system, and $\pi_i(j) = \Pr(S_i = j)$ means that the system is under state j when the i-th sampling packet arrives at the system.

1) The self-transfer between states has no contributions to the calculation of effective AoI since the new arrival samples are discarded in Phase 1 when the controller is busy. Therefore, the self-transfer between states is not shown in FGFS $M/M/1/1 \rightarrow M/M/1/2$ tandem queuing model.

If the new generated sampling packet can be accessed in the system, the above six Markov states can be summarized by the following three states:

1. "0": Phase 1 is idle, the actuator in Phase 2 is idle, and no control command is stored in the buffer, which is $(0,0)$ in Markov states;

2. "1": Phase 1 is idle, the actuator in Phase 2 is busy, and no control command is stored in the buffer, which is $(0,1)$ in Markov states;

3. "2": Phase 1 is idle, the actuator in Phase 2 is busy, and a control command is stored in the buffer, which is $(0,2)$ in Markov states.

To obtain the average EAoI for the n-th system update in control process, the following two conditions should hold: (1) in Phase 1, the $(n-1)$-th sampling packet should complete service before the n-th sampling packet arriving; (2) in Phase 2, the $(n-1)$-th corresponding control command packet should leave the controller and is performed at the actuator before the n-th corresponding control command packet arriving at the actuator. Then, the probability that the first sample arrives at the system and find that the system is under state "0" can be expressed as

$$\pi_1(0) = 1. \tag{2}$$

Then, the probability that the second sample arrives at the system and find that the system is under state "0" can be expressed as

$$\begin{aligned} \pi_2(0) &= \left(\frac{\mu_2}{\lambda+\mu_2}\right)\pi_1(0) \\ &= \frac{\mu_2}{\lambda+\mu_2}. \end{aligned} \tag{3}$$

For $n \geqslant 3$, the probability that the new sample arrives at the system and find that the system is under state "0" can be expressed as

$$\begin{aligned} \pi_n(0) &= \left(\frac{\mu_2}{\lambda+\mu_2}\right)\pi_{n-1}(0) + \left[\frac{\mu_2}{\lambda+\mu_2}\cdot\frac{\mu_2}{\mu_1+\mu_2} + \left(\frac{\mu_1}{\mu_1+\mu_2}\right)\cdot\left(\frac{\mu_2}{\lambda+\mu_2}\right)^2\right][1-\pi_{n-1}(0)] \\ &= \frac{\mu_2}{\lambda+\mu_2}\cdot\left[\left(1-\frac{\mu_1}{\mu_1+\mu_2}\cdot\frac{\lambda}{\lambda+\mu_2}\right) + \frac{\mu_1}{\mu_1+\mu_2}\cdot\frac{\lambda}{\lambda+\mu_2}\cdot\pi_{n-1}(0)\right] \\ &= \frac{\mu_2}{\lambda+\mu_2}\cdot\left(1-\frac{\mu_1}{\mu_1+\mu_2}\cdot\frac{\lambda}{\lambda+\mu_2}\right) + \frac{\mu_2}{\lambda+\mu_2}\cdot\frac{\mu_1}{\mu_1+\mu_2}\cdot\frac{\lambda}{\lambda+\mu_2}\cdot\pi_{n-1}(0). \end{aligned} \tag{4}$$

Based on (2), (3), and (4), we can obtain the average EAoI for each system update. For the first update, the average effective EAoI can be expressed as

$$\Delta_{1,1} = \frac{1}{\lambda} + \frac{1}{\mu_1} + \frac{1}{\mu_2}. \tag{5}$$

For the n-th update, the average EAoI can be expressed as

$$\begin{aligned} \Delta_{1,n} &= \left(\frac{1}{\lambda}+\frac{1}{\mu_1}+\frac{1}{\mu_2}\right)\pi_n(0) + \left[\frac{\mu_2}{\mu_1+\mu_2}\left(\frac{1}{\mu_1}+\frac{1}{\mu_2}\right) + \frac{1}{\mu_2}\frac{\mu_1}{\mu_1+\mu_2}\right](1-\pi_n(0)) \\ &= \left(\frac{1}{\lambda}+\frac{1}{\mu_1}+\frac{1}{\mu_2}\right)\pi_n(0) + \left(\frac{1}{\mu_1}+\frac{1}{\mu_2}-\frac{1}{\mu_1+\mu_2}\right)(1-\pi_n(0)) \\ &= \frac{1}{\mu_1}+\frac{1}{\mu_2}-\frac{1}{\mu_1+\mu_2} + \left(\frac{1}{\lambda}+\frac{1}{\mu_1+\mu_2}\right)\pi_n(0), \end{aligned} \tag{6}$$

where $n \geqslant 2$.

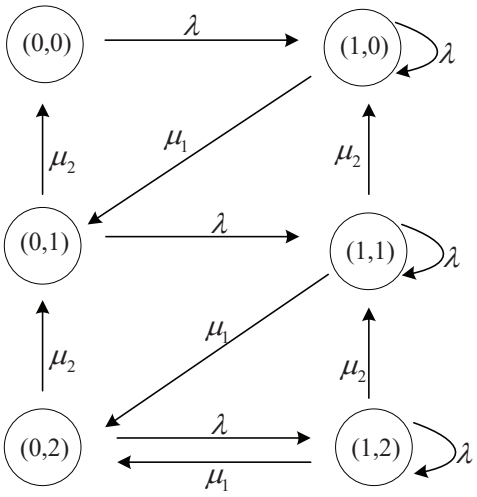

Figure 3 SHS Markov chain for $M/M/1/1^* \rightarrow M/M/1/2^*$ tandem queue.

3.2 Average EAoI for FGFS M/M/1/1* → M/M/1/2*

The states of FGFS $M/M/1/1^* \rightarrow M/M/1/2^*$ tandem queuing model are $(0,0)$ $(1,0)$ $(0,1)$ $(1,1)$ $(0,2)$ and $(1,2)$, where the entries in each state have the same meaning as that in FGFS $M/M/1/1 \rightarrow M/M/1/2$ tandem queuing model. The transition of the states can also be represented by SHS Markov chain, which is shown in Fig. 3.

For FGFS $M/M/1/1^* \rightarrow M/M/1/2^*$ tandem queuing model, the access into the system is significantly different from that in FGFS $M/M/1/1 \rightarrow M/M/1/2$ tandem queuing model. In FGFS $M/M/1/1^* \rightarrow M/M/1/2^*$, the samples are allowed to access when Phase 1 is either idle or busy. Furthermore, in Phase 2, the new generated control command can be transmitted to the actuator and served when the actuator is idle. On the other hand, the new generated control command should wait in the buffer when the actuator is busy. In summary, if the new generated sample can be accessed in Phase 1, the above six Markov states can be summarized by the following two states:

1. "0": Phase 1 is idle/busy, and the actuator is idle in Phase 2, which are $(0,0)$ and $(1,0)$ in Markov states;

2. "1": Phase 1 is idle/busy, and the actuator is busy in Phase 2, which are $(0,1)$, $(0,2)$, $(1,1)$, and $(1,2)$ in Markov states.

Then, the probability that the first sample arriving at the system and find that the system is under state "0" can be expressed as

$$\pi_1'(0) = 1. \tag{7}$$

Then, the probability that the second sample arriving at the system and find that the system is under state "0" can be expressed as

$$\begin{aligned} \pi_2'(0) &= \frac{\mu_2}{\lambda+\mu_2}\pi_1'(0) \\ &= \frac{\mu_2}{\lambda+\mu_2}. \end{aligned} \tag{8}$$

For $n \geqslant 3$, we have

$$\begin{aligned} \pi_n'(0) &= \left(\frac{\mu_2}{\lambda+\mu_2}\right)[\pi_{n-1}'(0) + \pi_{n-1}'(1)] \\ &= \left(\frac{\mu_2}{\lambda+\mu_2}\right)[\pi_{n-1}'(0) + (1 - \pi_{n-1}'(0))] \\ &= \frac{\mu_2}{\lambda+\mu_2} \end{aligned} \tag{9}$$

Based on (7), (8), and (9), we can obtain the average EAoI for each update in the control process. For the first update, the average EAoI can be expressed as

$$\Delta_{2,1} = \frac{1}{\lambda} + \frac{1}{\mu_1} + \frac{1}{\mu_2}. \tag{10}$$

For the n-th update, the average EAoI can be expressed as

$$\begin{aligned}\Delta_{2,n} &= (\frac{1}{\lambda} + \frac{1}{\mu_1} + \frac{1}{\mu_2})\pi'_n(0) + \left[\frac{\mu_2}{\mu_1+\mu_2}(\frac{1}{\mu_1} + \frac{1}{\mu_2}) + \frac{1}{\mu_2}\frac{\mu_1}{\mu_1+\mu_2}\right](1-\pi'_n(0)) \\ &= (\frac{1}{\lambda} + \frac{1}{\mu_1} + \frac{1}{\mu_2})\pi'_n(0) + \left(\frac{1}{\mu_1} + \frac{1}{\mu_2} - \frac{1}{\mu_1+\mu_2}\right)(1-\pi'_n(0)) \\ &= \frac{1}{\mu_1} + \frac{1}{\mu_2} - \frac{1}{\mu_1+\mu_2} + \left(\frac{1}{\lambda} + \frac{1}{\mu_1+\mu_2}\right)\pi'_n(0),\end{aligned} \tag{11}$$

where $n \geqslant 2$.

4 Throughput for Real-Time Wireless Feedback Control Systems

In this section, we investigate the system throughput based on the average EAoI for each system update in control process. Specifically, we first analyze system throughput in FGFS $M/M/1/1 \rightarrow M/M/1/2$ based on the average EAoI $\Delta_{1,n}$. Then, we study system throughput in FGFS $M/M/1/1^* \rightarrow M/M/1/2^*$ based on the average EAoI $\Delta_{2,n}$.

4.1 Throughput for FGFS M/M/1/1 → M/M/1/2

4.1.1 *Average EAoI Based Throughput*

Based on the average EAoI for each system update n in FGFS $M/M/1/1 \rightarrow M/M/1/2$, we can obtain the average total time $D_{1,n}$ elapsing in the system. When n is equal to 1, i.e., $n = 1$, we can obtain $D_{1,1}$ as

$$D_{1,1} = \Delta_{1,1} = \frac{1}{\lambda} + \frac{1}{\mu_1} + \frac{1}{\mu_2}. \tag{12}$$

Then, for $n \geqslant 2$, we have

$$\begin{aligned}D_{1,n} &= D_{1,n-1} + \Delta_{1,n} \\ &= D_{1,n-2} + \Delta_{1,n-1} + \Delta_{1,n} \\ &= D_{1,1} + \Delta_{1,2} + \cdots + \Delta_{1,n} \\ &= \Delta_{1,1} + \Delta_{1,2} + \cdots + \Delta_{1,n}.\end{aligned} \tag{13}$$

Substituting (5) and (6) into (13), $D_{1,n}$ can be obtained as

$$\begin{aligned}D_{1,n} &= \Delta_{1,1} + \Delta_{1,2} + \cdots + \Delta_{1,n} \\ &= n \cdot A + B\left(\sum_{i=1}^{n} \pi_n(0)\right),\end{aligned} \tag{14}$$

where

$$A = \frac{1}{\mu_1} + \frac{1}{\mu_2} - \frac{1}{\mu_1+\mu_2}, \tag{15}$$

and

$$B = \frac{1}{\lambda} + \frac{1}{\mu_1+\mu_2}. \tag{16}$$

Then, the system throughput can be obtained as

$$\begin{aligned}\rho_1 &= \lim_{n\to\infty} \frac{n}{D_{1,n}} \\ &= \lim_{n\to\infty} \frac{n}{n\cdot A + B\left(\sum_{i=1}^{n}\pi_n(0)\right)}.\end{aligned} \tag{17}$$

In (17), we have

$$\begin{aligned}\sum_{i=1}^{n}\pi_n(0) &= \pi_1(0)\frac{1-b^n}{1-b} - \frac{a}{1-b}\left(\frac{1-b^n}{1-b} - n\right) \\ &= \frac{1-b^n}{1-b} - \frac{a}{1-b}\left(\frac{1-b^n}{1-b} - n\right),\end{aligned} \tag{18}$$

where

$$a = \frac{\mu_2}{\lambda+\mu_2}\cdot\left(1 - \frac{\mu_1}{\mu_1+\mu_2}\cdot\frac{\lambda}{\lambda+\mu_2}\right), \tag{19}$$

and

$$b = \frac{\mu_2}{\lambda+\mu_2}\cdot\frac{\mu_1}{\mu_1+\mu_2}\cdot\frac{\lambda}{\lambda+\mu_2}. \tag{20}$$

Then, the system throughput in (17) can be further written as

$$\begin{aligned}\rho_1 &= \lim_{n\to\infty} \frac{n}{D_{1,n}} \\ &= \lim_{n\to\infty} \frac{n}{n\cdot A + B\left(\frac{1-b^n}{1-b} - \frac{a}{1-b}\left(\frac{1-b^n}{1-b} - n\right)\right)} \\ &= \frac{1}{A + B\cdot\frac{a}{1-b}}.\end{aligned} \tag{21}$$

From the above discussion, the system throughput is determined by the accumulation of the average EAoI for each system update in the control process. Next, we analyze the relationship between the throughput and the update rate μ_1 in Phase 1 and μ_2 in Phase 2.

4.1.2 *Relationship Between Throughput and Update Rate in EAoI*

We assume the throughput is represented by $\rho_{1,1}$ when the update rate μ_1 for Phase 1 is greater than the update rate μ_2 for Phase 2, i.e., $\mu_1 > \mu_2$. On the contrary, the throughput is represented by $\rho_{1,2}$ when the update rate μ_1 for Phase 1 is less than or equal to the update rate μ_2 for Phase 2, i.e., $\mu_1 \leqslant \mu_2$. Then, from (21), we have

$$\begin{aligned}\frac{1}{\rho_{1,1}} - \frac{1}{\rho_{1,2}} &= (A_1 - A_2) + \left(B_1\frac{a_1}{1-b_1} - B_2\frac{a_2}{1-b_2}\right) \\ &= B_1\left(\frac{a_1}{1-b_1} - \frac{a_2}{1-b_2}\right),\end{aligned} \tag{22}$$

where $A_1 = A_2 = \frac{1}{\mu_1} + \frac{1}{\mu_2} - \frac{1}{\mu_1+\mu_2}$, $B_1 = B_2 = \frac{1}{\lambda} + \frac{1}{\mu_1+\mu_2}$, $a_1 = \frac{\mu_2}{\lambda+\mu_2}\cdot\left(1 - \frac{\mu_1}{\mu_1+\mu_2}\cdot\frac{\lambda}{\lambda+\mu_2}\right)$, $a_2 = \frac{\mu_1}{\lambda+\mu_1}\cdot\left(1 - \frac{\mu_2}{\mu_1+\mu_2}\cdot\frac{\lambda}{\lambda+\mu_1}\right)$, $b_1 = \frac{\mu_2}{\lambda+\mu_2}\cdot\frac{\mu_1}{\mu_1+\mu_2}\cdot\frac{\lambda}{\lambda+\mu_2}$, and $b_2 = \frac{\mu_1}{\lambda+\mu_1}\cdot\frac{\mu_2}{\mu_1+\mu_2}\cdot\frac{\lambda}{\lambda+\mu_1}$.

In (22), we have

$$\begin{aligned}\frac{1-b_1}{a_1} - \frac{1-b_2}{a_2} &= \left(1 - \frac{\mu_2}{\lambda+\mu_2}\cdot\frac{\mu_1}{\mu_1+\mu_2}\cdot\frac{\lambda}{\lambda+\mu_2}\right)\frac{\lambda+\mu_2}{\mu_2} - \left(1 - \frac{\mu_1}{\lambda+\mu_2}\cdot\frac{\mu_2}{\mu_1+\mu_2}\cdot\frac{\lambda}{\lambda+\mu_1}\right)\frac{\lambda+\mu_1}{\mu_1} \\ &= \frac{\lambda(\mu_1-\mu_2)}{\mu_1\mu_2} + \frac{\lambda}{\mu_1+\mu_2}\left(\frac{\mu_2}{\lambda+\mu_1} - \frac{\mu_1}{\lambda+\mu_2}\right) \\ &= \frac{\lambda^2(\mu_1^2-\mu_2^2) + \lambda(\mu_1^3-\mu_2^3) + 2\lambda\mu_1\mu_2(\mu_1-\mu_2) + 2\mu_1\mu_2(\mu_1^2-\mu_2^2)}{\mu_1\mu_2(\mu_1+\mu_2)(\lambda+\mu_1)(\lambda+\mu_2)}.\end{aligned} \tag{23}$$

Then, we can obtain $\frac{1-b_1}{a_1} - \frac{1-b_2}{a_2} > 0$ and $\frac{1}{\rho_{1,1}} - \frac{1}{\rho_{1,2}} < 0$ in (22), which means that $\rho_{1,1} > \rho_{1,2}$. According to the update rates for Phase 1 and 2, we have the following two cases:

1. Case I: update rate μ_1 for Phase 1 is greater than update rate μ_2 for Phase 2, i.e., $\mu_1 > \mu_2$;

2. Case II: update rate μ_1 for Phase 1 is less than or equal to update rate μ_2 for Phase 2, i.e., $\mu_1 \leqslant \mu_2$.

Then,the following property can be obtained.

Property 1. *In real-time wireless feedback control systems with $M/M/1/1 \rightarrow M/M/1/2$ tandem queuing model, the average system throughput for Case I is greater than that for Case II. Furthermore, since average throughput is accumulated by inverse of the average EAoI for each system update in the control process, the average EAoI for Case I is less than that for Case II.* ■

4.2 Throughput for FGFS M/M/1/1* → M/M/1/2*

4.2.1 *Average EAoI Based Throughput*

Based on the average EAoI for each system update n in FGFS $M/M/1/1^* \rightarrow M/M/1/2^*$, we can obtain the average total time $D_{2,n}$ elapsing from the system. For the first update, i.e., $n = 1$, we can obtain $D_{2,1}$ as

$$D_{2,1} = \Delta_{2,1} = \frac{1}{\lambda} + \frac{1}{\mu_1} + \frac{1}{\mu_2}. \tag{24}$$

Then, for $n \geqslant 2$, we have

$$D_{2,n} = \Delta_{2,1} + \Delta_{1,2} + \cdots + \Delta_{2,n}. \tag{25}$$

Substituting (10) and (11) into (25), we can obtain $D_{2,n}$ as

$$D_{2,n} = n \cdot A + B\left(\sum_{i=1}^{n} \pi'_n(0)\right), \tag{26}$$

where A and B is obtained in (15) and (16), respectively. Then, the system throughput can be obtained as

$$\begin{aligned} \rho_2 &= \lim_{n\to\infty} \frac{n}{D_{2,n}} \\ &= \lim_{n\to\infty} \frac{n}{n \cdot A + B\left(\sum_{i=1}^{n} \pi'_n(0)\right)}. \end{aligned} \tag{27}$$

In (27), we have

$$\sum_{i=1}^{n} \pi'_n(0) = \frac{\lambda + n\mu_2}{\lambda + \mu_2}. \tag{28}$$

Then, the system throughput in (27) can be further written as

$$\begin{aligned} \rho_2 &= \lim_{n\to\infty} \frac{n}{n \cdot A + B\left(\frac{\lambda+n\mu_2}{\lambda+\mu_2}\right)} \\ &= \frac{1}{A + B \cdot \frac{\mu_2}{\lambda+\mu_2}}. \end{aligned} \tag{29}$$

Similar with FGFS $M/M/1/1 \rightarrow M/M/1/2$, the system throughput in FGFS $M/M/1/1^* \rightarrow M/M/1/2^*$ is also determined by the accumulation of EAoI. Next, we analyze the relationship between the throughput and update rate μ_1 and μ_2.

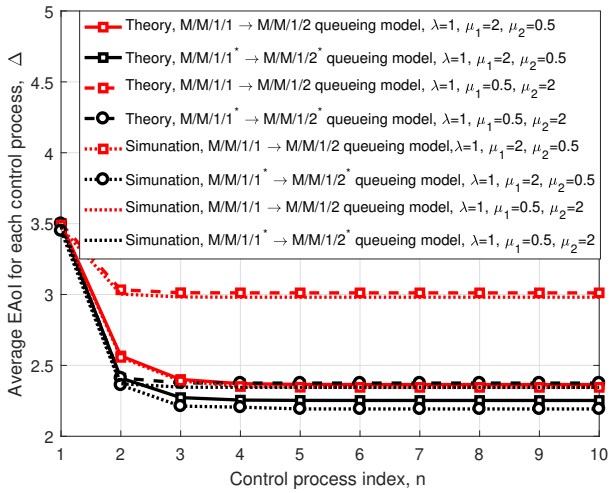

Figure 4 Average EAoI for each system update n in the control process with different tandem queuing models.

4.2.2 *Relationship Between Throughput and Update Rate in EAoI*

We assume the throughput is represented by $\rho_{2,1}$ when the update rate μ_1' for Phase 1 is greater than the update rate μ_2' for Phase 2, i.e., $\mu_1' > \mu_2'$. On the contrary, the throughput is represented by $\rho_{2,2}$ when the update rate μ_1' for Phase 1 is less than or equal to the update rate μ_2' for Phase 2, i.e., $\mu_1' \leqslant \mu_2'$. Then, from (29), we have

$$\frac{1}{\rho_{2,1}} - \frac{1}{\rho_{2,2}} = B_1'\left(\frac{\mu_2'}{\lambda+\mu_2'} - \frac{\mu_1'}{\lambda+\mu_1'}\right), \tag{30}$$

where $B_1' = \frac{1}{\lambda} + \frac{1}{\mu_1'+\mu_2'}$. In (30), we have

$$\frac{\mu_2'}{\lambda+\mu_2'} - \frac{\mu_1'}{\lambda+\mu_1'} < 0. \tag{31}$$

When $\mu_1' > \mu_2'$, we can obtain $\frac{1}{\rho_{2,1}} - \frac{1}{\rho_{2,2}} < 0$ in (30), which means that $\rho_{2,1} > \rho_{2,2}$. Based on the above discussion, the following property can be obtained for FGFS $M/M/1/1^* \rightarrow M/M/1/2^*$, which is the same with $M/M/1/1 \rightarrow M/M/1/2$ tandem queuing model in Property 1.

Property 2. *In real-time wireless feedback control systems with $M/M/1/1^* \rightarrow M/M/1/2^*$ tandem queuing model, the average system throughput for Case I is greater than that for Case II. Furthermore, since average throughput is accumulated by inverse of the average EAoI, the average EAoI for Case I is less than that for Case II.* ■

5 Numerical Results

In this section, we provide numerical results to demonstrate the average EAoI and its relationship with the overall system throughput in real-time wireless feedback control systems. For the adopted FCFS $M/M/1/1 \rightarrow M/M/1/2$ tandem queuing model and FCFS $M/M/1/1^* \rightarrow M/M/1/2^*$ tandem queuing model, we assume that the arrival rate of Poisson process for samples is $\lambda = 1$. Furthermore, the update rates μ_1 and μ_2 are variables according to different performance simulations.

Fig. 4 shows the performance of average EAoI for each system update n in control process with different tandem queuing models given different update rates μ_1 and μ_2. From the figure, all four curves with different μ_1 and μ_2 first decrease and then maintain horizontal with n increasing for both $M/M/1/1 \rightarrow M/M/1/2$ tandem queuing model and $M/M/1/1^* \rightarrow M/M/1/2^*$ tandem queuing model. The average EAoI in either (6) for $M/M/1/1 \rightarrow M/M/1/2$ or (11) for $M/M/1/1^* \rightarrow M/M/1/2^*$ changes with the probability $\pi_n(0)$ or $\pi_n'(0)$ linearly. At the first three system updates, i.e., $n \leqslant 3$, both $\pi_n(0)$ and $\pi_n'(0)$ would decrease. Then, the system is stable when $n > 3$, where both $\pi_n(0)$ and $\pi_n'(0)$ would be constant. Thus, the changes of the four curves with system update n are reasonable. Furthermore, considering

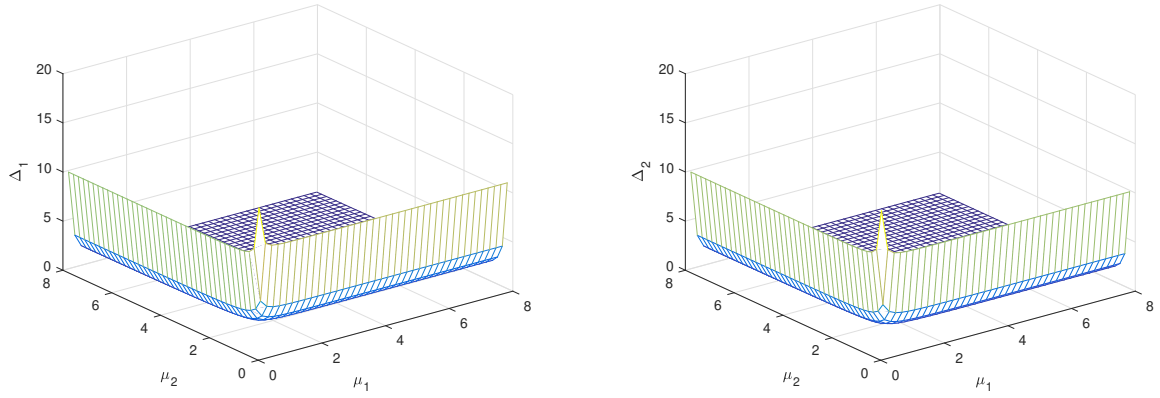

Figure 5 Average EAoI for system update $n = 5$ in different tandem queuing models with different update rate μ_1 and μ_2 (a) Average EAoI for system update $n = 5$ in $M/M/1/1 \rightarrow M/M/1/2$ tandem queuing model; (b)Average EAoI for system update $n = 5$ in $M/M/1/1^* \rightarrow M/M/1/2^*$ tandem queuing model

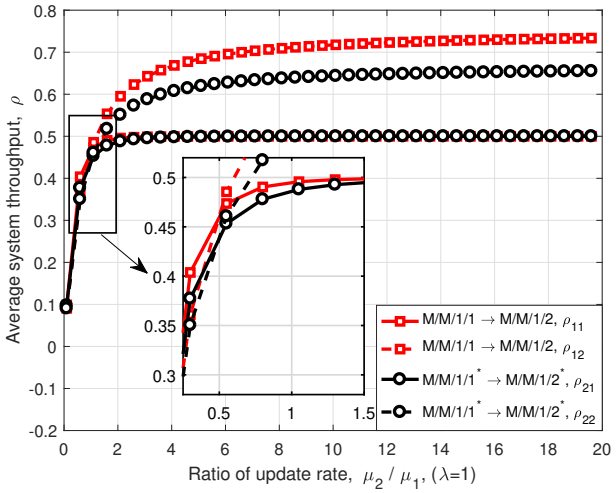

Figure 6 Average throughput with different ratio μ_2/μ_1 for different queuing models.

$n > 3$, e.g., $n = 5$, the average EAoI of the case when $\mu_1 > \mu_2$ is smaller than that when $\mu_1 < \mu_2$ for the both two adopted tandem queuing models. The reason can be obtained by comparing the (6) (or (11)) with different assumptions $\mu_1 > \mu_2$ and $\mu_1 < \mu_2$, which are also corresponding with the **Property 1** and **2**, i.e., the average EAoI when $\mu_1 > \mu_2$ is less than that when $\mu_1 < \mu_2$. In addition, comparing the curves with the same μ_1 and μ_2 for $M/M/1/1 \rightarrow M/M/1/2$ tandem queuing model and $M/M/1/1^* \rightarrow M/M/1/2^*$ tandem queuing model, e.g., $\mu_1 = 2$ and $\mu_2 = 0.5$, the curve of $M/M/1/1^* \rightarrow M/M/1/2^*$ tandem queuing model is below that of $M/M/1/1 \rightarrow M/M/1/2$ tandem queuing model, which indicates that $M/M/1/1^* \rightarrow M/M/1/2^*$ tandem queuing model outperforms $M/M/1/1 \rightarrow M/M/1/2$ tandem queuing model in terms of EAoI. Furthermore, the comparison of the theory results and numerical results is shown in this figure, where the performance loss is minor and can be ignored. In the following of this section, we use the theory results to show the performance of the proposed method.

Fig. 5 illustrates the performance of the average EAoI for system update $n = 5$ in different tandem queuing models with different update rate μ_1 and μ_2, where average EAoIs Δ_1 and Δ_2 are shown in Fig. 5(a) and Fig. 5(b) for $M/M/1/1 \rightarrow M/M/1/2$ tandem queuing model and $M/M/1/1^* \rightarrow M/M/1/2^*$ tandem queuing model, respectively. From the figure, the average EAoIs strictly decrease with increasing μ_1 and μ_2. Furthermore, when μ_1 and μ_2 are large enough, the average EAoIs Δ_1 and Δ_2 would be stable with little changes. This is reasonable since both (6) and (11) would be constant when $\mu_1 \rightarrow \infty$ and $\mu_2 \rightarrow \infty$.

Fig. 6 shows the performance of average throughput with different ratio of update rates μ_2/μ_1 for

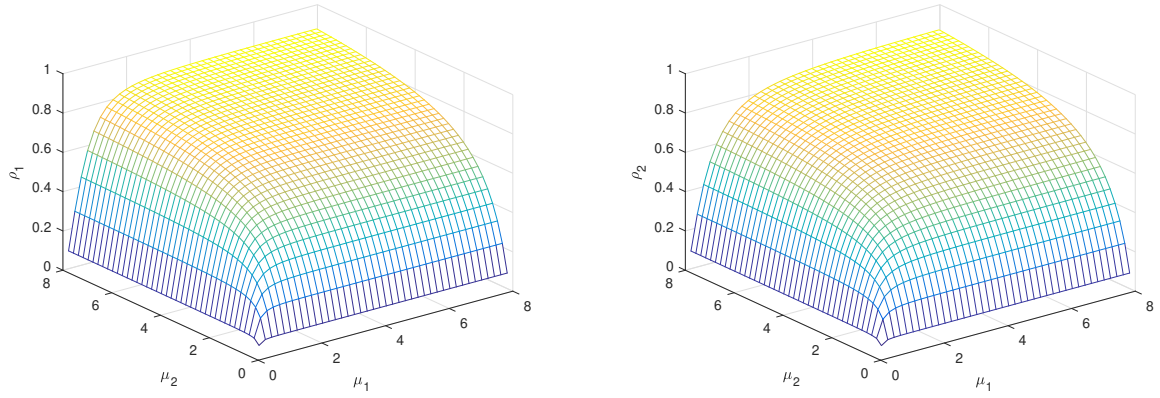

Figure 7 Average throughput for different tandem queuing models with different process rate μ_1 and μ_2 (a) Average throughput for $M/M/1/1 \rightarrow M/M/1/2$ tandem queuing model; (b)Average throughput for $M/M/1/1^* \rightarrow M/M/1/2^*$ tandem queuing model

different tandem queuing models, where we have $\lambda = 1$. From the figure, all throughput curves first increase with respect to μ_2/μ_1 ratio, then reach a saturate value when the ratio is large enough for both $M/M/1/1 \rightarrow M/M/1/2$ tandem queuing model and $M/M/1/1^* \rightarrow M/M/1/2^*$ tandem queuing model. This is reasonable since both (21) and (29) would be constant when μ_1 and μ_2 are large enough. In addition, when $\mu_2 < \mu_1$, i.e., $\mu_2/\mu_1 < 1$, the throughput of Case I (i.e., the rate of Phase 1 being higher than the rate of Phase 2) is higher than that of Case II (i.e., the rate of Phase 1 being smaller than the rate of Phase 2) for the two queuing models. The reason can be obtained by the **Property 1** and **Property 2**. On the other hand, when $\mu_2 > \mu_1$, i.e., $\mu_2/\mu_1 > 1$, the throughput of Case I is smaller than that of Case II. When the throughput is stable and saturate, we can obtain that the performance gains of Case II are about 50% and 35% compared with Case I for $M/M/1/1 \rightarrow M/M/1/2$ and $M/M/1/1^* \rightarrow M/M/1/2^*$ tandem queuing models, respectively.

Furthermore, in Fig. 6, given λ, μ_1, and μ_2, the throughput of the $M/M/1/1^* \rightarrow M/M/1/2^*$ tandem queuing model is smaller than that of the $M/M/1/1 \rightarrow M/M/1/2$ tandem queuing model, because the throughput is the inverse of the accumulation of the EAoI. Therefore, the relationship of throughput is in contrast to the EAoI for the two models.

Fig. 7 illustrates the performance of average throughput for different tandem queuing models with different process rate μ_1 and μ_2, where average throughput ρ_1 and ρ_2 are shown in Fig. 7(a) and Fig. 7(b) for $M/M/1/1 \rightarrow M/M/1/2$ tandem queuing model and $M/M/1/1^* \rightarrow M/M/1/2^*$ tandem queuing model, respectively. From the figure, the average throughput in both Fig. 7(a) and Fig. 7(b) increases with μ_1 and μ_2. Furthermore, when μ_1 and μ_2 are large enough, the average throughput ρ_1 and ρ_2 would be stable with minor changes, where the reason is the same as that in Fig. 5.

6 Conclusions

In this paper, the Effective Age of Information (EAoI) is proposed for real-time wireless control systems which is a critical metric since it indicates both latency and packet loss in URLLC. To describe the whole process from sensor to actuator, we adopted two first-generate-first-serve (FGFS) tandem queuing models, i.e., FGFS $M/M/1/1 \rightarrow M/M/1/2$ tandem queuing model and FGFS $M/M/1/1^* \rightarrow M/M/1/2^*$ tandem queuing model, where the difference between them is that the new arrival packet would replace the existing packet in FGFS $M/M/1/1^* \rightarrow M/M/1/2^*$ tandem queuing model. Then, the stochastic hybrid system Markov chain was introduced to analyze the two tandem queuing models. Based on that, we calculated EAoI for each system update. More importantly, we analyzed the relationship between system throughput and EAoI. This provides a guideline for URLLC system design in real-time feedback control systems: (1) both update rates μ_1 in Phase 1 and μ_2 in Phase 2 should be large to reduce EAoI; (2) μ_2 should be larger than μ_1 to increase the system throughput; (3) there is minor effect on EAoI and throughput when μ_1 and μ_2 are larger than a certain threshold. As a future work, optimization of update rates will be studied using proposed EAoI metric to achieve certain level of performance in real-time wireless feedback control systems. In addition, the tail behaviour of the AoI may also be useful

to represent extreme situations in some scenarios. However, it is extremely challenging to analyze the tail behaviour in tandem queueing model. Therefore, addressing this issue would be our future work. Design aspects of the proposed metric are also crucial for system design and system performance. One of the main design difficulty could be the time synchronization of the two phases of the control process to effectively use the proposed EAoI metric since, the first phase and the second phase of the control process take place in different physical locations.

Acknowledgements A part of this work is supported by the National Natural Science Foundation of China under Grant 61631004.

References

1 C. Lu, A. Saifullah, B. Li, M. Sha, H. Gonzalez, D. Gunatilaka, C. Wu, L. Nie, and Y. Chen, "Real-time wireless sensor-actuator networks for industrial cyber-physical systems," *Proc. the IEEE*, vol. 104, no. 5, pp. 1013-1024, May 2016.

2 K. Sato, Y. Kawamoto, H. Nishiyama, N. Kato, and Y. Shimizu, "A modeling technique utilizing feedback control theory for performance evaluation of IoT system in real-time," *International Conf. Wireless Commun. & Signal Processing (WCSP)*, pp. 1-5, Oct. 2015.

3 T. Hößler, M. Simsek, and G. P. Fettweis, "Mission reliability for URLLC in wireless networks," *IEEE Communications Letters*, vol. 22, no. 11, pp. 2350-2353, Nov. 2018.

4 B. Singh, O. Tirkkonen, Z. Li, and Mikko A. Uusitalo, "Contention-based access for ultra-reliable low latency uplink transmissions," *IEEE Wireless Commun. Lett.*, vol. PP, no. 99, pp. 1-4, Oct. 2017.

5 J. Nielsen, R. Liu, and P. Popovski, "Ultra-reliable low latency communication (URLLC) using interface diversity," *IEEE Trans. Commun.*, vol. 66, no. 3, pp. 1322-1334, Mar. 2018.

6 C. She, C. Yang, and T. Quek, "Radio resource management for ultra-reliable and low-latency communications," *IEEE Commun. Mag.*, vol. 55, no. 6, pp. 72-78, Jun. 2017.

7 C. She, C. Yang, and T. Quek, "Cross-layer optimization for ultra-reliable and low-latency radio access networks," *IEEE Trans. Wireless Commun.*, vol. PP, no. 99, pp. 1-15, Oct. 2017.

8 H. Geng and P. Alto, *Internet of Things and Data Analytics Handbook*, Wiley Press, 2016.

9 3GPP TR 22804, *Study on Communication for Automation in Vertical Domains*, Dec. 2018.

10 B. Chang, L. Zhang, L. Li, G. Zhao, and Z. Chen, "Optimizing resource allocation in URLLC for real-time wireless control systems," *IEEE Trans. Vehicular Technology*, vol. 68, no. 9, pp. 8916-8927, Sept. 2019.

11 B. Chang, G. Zhao, Z. Chen, L. Li, and M. A. Imran, "Packet-drop design in URLLC for real-time wireless control systems," *IEEE Access*, vol. 7, pp. 1-10, Jul. 2019.

12 B. Chang, G. Zhao, L. Zhang, M. A. Imran, Z. Chen, and L. Li, "Dynamic communication QoS design for real-time wireless control systems," *IEEE Sensors Journal*, vol. 20, no. 6, pp. 1-10, Mar. 2020.

13 B. Chang, G. Zhao, Z. Chen, P. Li, and L. Li, "D2D transmission scheme in URLLC enabled real-time wireless control systems for tactile internet," *IEEE GLOBECOM*, pp. 1-6, Dec. 2019.

14 M. Costa, M. Codreanu, and A. Ephremides, "On the age of information in status update systems with packet management," *IEEE Trans. Information Theory*, vol. 62, no. 4, pp. 1897-1910, Apr. 2016.

15 S. Kaul, M. Gruteser, V. Rai, and J. Kenney,"Minimizing age of information in vehicular networks," in *IEEE Conf. Sensor, Mesh and Ad Hoc Communications and Networks (SECON)*, Jun. 2011, pp. 1-9.

16 E. G. Coffman Jr, Z. Liu, and R. R. Weber, "Optimal robot scheduling for web search engines," *Journal of scheduling*, vol. 1, no. 1, pp. 15–29, 1998.

17 J. Cho and H. Garcia-Molina, "Synchronizing a database to improve freshness," *ACM sigmod record*, vol. 29, no. 2, pp. 117–128, 2000.

18 B. Chang, L. Li, G. Zhao, Z. Meng, M. A. Imran, and Z. Chen, "Age of information for actuation update in real-time wireless control systems," in *3rd IEEE INFOCOM Age of Information Workshop*, Jul. 2020.

19 S. Kaul, R. Yates, and M. Gruteser, "Real-time status: How often should one update?," in Proc. *IEEE Infocom*, May, 2011, pp. 2731-2735.

20 C. Kam, S. Kompella, and A. Ephremides, "Age of information under random updates," *IEEE Inter. Sym. Infor.Theory (ISIT)*, Jul. 2013, pp. 66-70.

21 S. Kaul, R. Yates, and M. Gruteser, "Status updates through queues," in *Proc. Conf. Inf. Sci. Syst. (CISS)*, Mar. 2012, pp. 1-6.

22 S. Kaul, R. Yates, and M. Gruteser, "Real-time status: How often should one update?" in *Proc. IEEE INFOCOM*, Mar. 2012, pp. 2731-2735.

23 Y. Sun, E. Biyikoglu, R. Yates, C. Koksal, and N. Shroff, "Update or wait: how to keep your data fresh," *IEEE Trans. Information Theory*, vol. 63, no. 11, pp. 7492-7508, Nov. 2017.

24 B. Bancinoglu, Y. Sun, E. Uysal, and V. Mutlu, "Optimal status updating with a finite-battery energy harvesting source," *arXiv preprint arXiv:1905.06679*, pp, 1-15, May 2019.

25 J. Zhong, R. Yates, and E. Soljanin, "Timely lossless source coding for randomly arriving symbols," *IEEE Information Theory Workshop (ITW)*, Nov. 2018, pp. 1-5.

26 R. Yates, P. Ciblat, A. Yener, and M. Wigger, "Age-optimal constrained cache updating," *IEEE Inter. Sym. Information Theory (ISIT)*, Jun. 2017, pp. 141-145.

27 T. Ornee and Y. Sun, "Sampling for remote estimation through queues: age of information and beyond," *arXiv preprint arXiv:1902.03552*, pp. 1-17, Jun. 2019.

28 H. Yang, A. Arafa, T. Quek, and H. V. Poor, "Age-based scheduling policy for federated learning in mobile edge networks," *arXiv preprint arXiv:1910.14648*, Oct, 2019.

29 X. Zheng, S. Zhou, and Z. Niu, "Context-aware information lapse for timely status updates in remote control systems," *arXiv preprint arXiv:1908.04446*, Aug. 2019.

30 O. Ayan, M. Vilgelm, M. Klugel, S. Hirche, and W. Kellerer, "Age-of-information vs. value-of-information scheduling for cellular networked control systems," *ACM/IEEE Inter. Conf. Cyber-Physical Systems*, Apr. 2019, pp. 109-117.

31 J. Champati, M. Mamduhi, K. Johansson, and J. Gross, "Performance characterization using aoi in a single-loop networked control system," *arXiv preprint arXiv:1901.06694*, 2019.

32 O. Ayan, M. Vilgelm, and W Kellerer, "Optimal scheduling for discounted age penalty minimization in multi-loop networked control," *arXiv preprint arXiv:1908.01503*, 2019.

33 J. Zhang and C. Wang, "On the rate-cost of gaussian linear control systems with random communication delays," *IEEE ISIT*, pp. 2441-2445, Jun. 2018.

34 R. Yates and S. Kaul, "The age of information: real-time status updating by multiple sources," *IEEE Trans. Infor. Theory*, vol. 65, no. 3, pp. 1807-1827, Mar. 2019.

35 C. Kam, J. Molnar, and S. Kompella, "Age of information for queues in tandem," *IEEE Military Commun. Conf. (MILCOM)*, Oct. 2018, pp. 462-467.

36 B. Demirel, V. Gupta, D. Quevedo, and M. Johansson, "On the trade-off between communication and control cost in event-triggered dead-beat control," *IEEE Trans. Automatic Control*, vol. 62, no. 6, pp. 2973-2980, Jun. 2017.

37 G. Klančar and I. Škrjanc, "Tracking-error model-based predictive control for mobile robots in real time," *Robotics and autonomous systems*, vol. 55, no. 6, pp. 460-469, 2007.

38 J. Shortle, J. Thompson, D. Gross, and C. Harris, *Fundamentals of queueing theory (fifth edition)*, Wiley Press, 2018.